ICRC 2001

The acceleration and transport of test particles in hydrodynamical simulations

P. Duffy[1]**, V. V. Dwarkadas**[2]**, and Lewis Ball**[3]

[1]Department of Mathematical Physics, U.C.D., Dublin 4, Ireland
[2]Bartol Research Institute, University of Delaware, Newark, DE19716, USA
[3]RCfTA, School of Physics, University of Sydney, NSW 2006, Australia

Abstract. The interaction of supernovae with their surroundings has been studied with hydrodynamical codes which capture the shock waves produced when the ejecta interact with the medium close to the progenitor star. Observationally it is known that core-collapse supernovae, of which SN1987A and SN1993J are two well-studied examples, emit nonthermal radiation which is associated with electron acceleration at these shock waves. We present a model for the transport and acceleration of test particles in hydrodynamical simulations of young radio supernovae.

1 Introduction

Multidimensional hydrodynamical codes are widely used to study the ejecta from a supernova explosion and their interaction with the circumstellar environment (e.g. Blondin & Lundqvist 1993; Jun & Jones 1999; Dwarkadas 2000). These simulations allow us to picture the complex interaction between the matter ejected in the explosion and the surrounding medium. Young supernovae arising from core collapse, such as SN1987A and SN1993J, are also observed as radio synchrotron sources, implying the presence of energetic electrons. These particles are believed to be accelerated at the shock front between the ejecta and the undisturbed external medium, before being advected downstream where they undergo adiabatic losses. This physical process is not generally included in purely hydrodynamical simulations (see however Jun & Jones 1999), which are therefore difficult to compare with detailed radio observations. In this paper we propose a simple computational model which takes the data output from a hydrodynamical simulation and uses it to solve for the electron acceleration and transport.

The electron population is described by a kinetic transport equation which includes the effects of advection, diffusion and adiabatic losses. The solution of this equation is computationally intensive, particularly when more than one spatial

Correspondence to: P. Duffy (peter.duffy@ucd.ie)

dimension is relevant, even in the test particle approximation where a given level of plasma turbulence is assumed. The inclusion of energetic nucleons, which can modify the shock structure, is a further complication. Ultimately we aim to complete the following steps for multi-dimensional flows:

– Take the data from a hydrodynamical simulation, on relatively coarse spatial and temporal scales if necessary, and use them to calculate the evolving distribution of energetic electrons.
– Model the evolution of the postshock magnetic field in order to construct synthetic radio images of the source.
– Include the effect of energetic nucleons on the hydrodynamics, as in Duffy, Ball & Kirk (1995), from which the electron population and radio emission is calculated.

In this paper we discuss a method to perform the first of these steps in a one-dimensional, spherically symmetric system. Section 2 outlines the hydrodynamical method used, section 3 details the electron transport and acceleration scheme, and the results are discussed in section 4.

2 Hydrodynamics

The simulations described herein were carried out using the VH-1 code, a one, two or 3-dimensional code based on the Piecewise Parabolic Method of Colella and Woodward (1984). This shock-capturing code works by solving the Riemann problem at each zone interface, and uses parabolic (rather than linear) interpolation for the variables. In order to track the shock velocities at various zones at successive timesteps, a grid of fixed size was used employing a very large number of zones, typically 10000 to 15000.

The nature of the ejecta density distribution of Type II supernovae is not well known. Explosion models for the progenitor of SN1987A appear to indicate that the density falls off with radius approximately as a power-law with index close to -9 (i.e. $\rho \propto r^{-9}$; Luo, McCray & Slavin 1994). Power-law density profiles are quite commonly used in modelling, if only because the interaction of a supernova with a
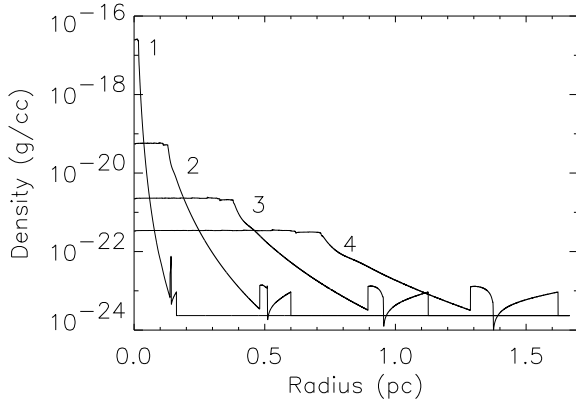
Fig. 1. Density profiles for an explosion in a constant density environment, at four epochs; 1: 5.2yr, 2: 40.6yr, 3: 119.0yr, 4: 224.0yr.

Fig. 2. Velocity profiles for an explosion in a constant density environment, at epochs 1: 5.2yr, 2: 40.6yr, 3: 119.0yr, 4: 224.0yr.

power-law density profile with a surrounding medium whose density also decreases as a power-law with radius can be described by an analytic, self-similar solution (Chevalier 1982). As a starting point we describe the ejecta density by a power-law with an index of -7. Since the ejected mass and energy of the explosion must be finite, the power-law cannot extend back to zero radius. Typically the density is taken to be uniform for ejecta velocities below a certain transition velocity, which can be computed from the ejected mass and energy of the explosion.

Core-collapse supernovae arise from massive stars. As the star evolves through the HR diagram, a wind driven off by it may appreciably alter the surrounding medium. When the star explodes as a supernova, the resulting shock wave will interact, at least initially, with this modified circumstellar medium. If the wind properties are constant, the density of the surrounding medium will fall off as r^{-2}. We examine both this case and the situation where the supernova expands into a constant density interstellar medium unaffected by a wind from the progenitor. In the latter case we assume $\rho = 2.34 \times 10^{-24}$ g cm^{-3}, appropriate for an interstellar medium with a 10:1 ratio of H:He.

The simulations are initiated by assuming an appropriate ejecta density profile up to a contact radius, beyond which the density profile is that of the surrounding medium undisturbed by the explosion. The initial contact radius can be obtained from the self-similar solution. The expansion of the supernova ejecta into the surrounding medium gives rise to two shocks separated by a contact discontinuity. The outer shock expands into the ambient medium. The inner shock also moves outwards initially, but it does so more slowly than the fastest ejecta. The region between the inner (reverse) shock and the contact discontinuity consists of shocked ejecta, and the ambient medium is shocked and swept up into a shell between the outer shock and the contact discontinuity.

Figures 1 and 2 show representative plots of the density and velocity profiles respectively, at four different epochs,
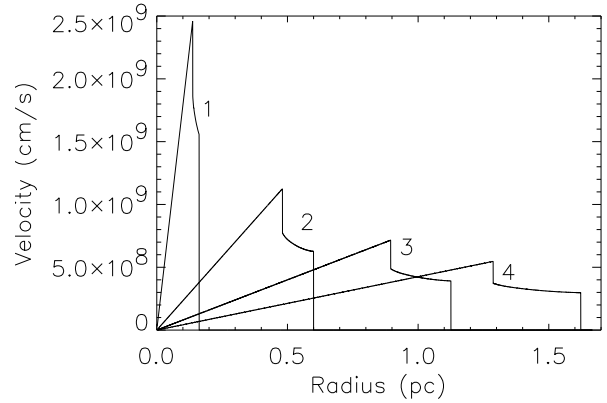
for expansion into a constant density medium. Figures 3 and 4 display the corresponding results for an explosion in a medium with density $\propto r^{-2}$. In both cases the double shock structure is clearly evident in the density and velocity plots at the later three epochs. Both shocks are strong, with a density jump of 4. The self-similar nature of the expansion is apparent; the shape of the double shocked structure remains essentially the same while it increases in size. The density at the contact discontinuity drops asymptotically to zero for expansion into a constant density medium, and rises to infinity for the wind case. The velocity does not change across the contact discontinuity, and there is little difference between the velocity profiles in the two cases.

3 Electron transport and acceleration

In the presence of MHD waves, which are advected with the flow and which scatter and isotropise energetic particles, the transport equation for the electron phase space density $f(\mathbf{r}, p, t)$ is

$$\frac{\partial f}{\partial t} + \mathbf{v} \cdot \nabla f = \nabla \kappa \nabla f + \frac{1}{3} \nabla \cdot \mathbf{v} p \frac{\partial f}{\partial p} \quad (1)$$

where $\mathbf{v}(\mathbf{r}, t)$ is the bulk fluid flow velocity and κ is the particle diffusion coefficient. While it is possible in principle to solve this full kinetic equation using flow data from a hydrodynamical simulation, such an approach is computationally intensive compared to solving the fluid equations because of the extra dependence on the particle momentum. To reduce the computational burden we adopt an approach used in previous work (e.g. Ball & Kirk 1992) in which acceleration and transport are effectively separated.

We consider electrons which diffuse, with coefficient κ, around a shock front because of scattering by magnetic structures advected with the flow. The scattering ensures that the electron distribution remains almost isotropic. In the rest frame of the forward shock the upstream flow speed at a
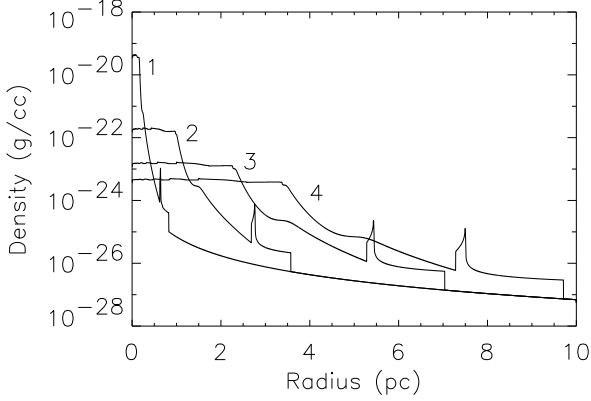
Fig. 3. Density profiles for an explosion in a wind with density $\propto r^{-2}$, at epochs 1: 47.4yr, 2: 288.8yr, 3: 669.0yr, 4: 998.0yr.

Fig. 4. Velocity profiles for an explosion in a wind with density $\propto r^{-2}$, at epochs 1: 47.4yr, 2: 288.8yr, 3: 669.0yr, 4: 998.0yr.

given instant is denoted by v_1 and that downstream of the shock by v_2. These speeds are computed from the results of the hydrodynamical simulation. In the box model of Drury et al. (1999) only particles within a diffusive lengthscale,

$$L = \kappa \left(\frac{1}{v_1} + \frac{1}{v_2} \right) , \qquad (2)$$

of the shock interact effectively with it. The differential number of particles of momentum p in the box is $4\pi p^2 f_s L$, where $f_s(p,t)$ the momentum space distribution of particles in the shock's vicinity averaged over the box size L. These particles are scattered back and forth across the shock by the magnetic turbulence and there is a flux of particles upwards in momentum at the shock given by

$$\Phi = \frac{4\pi p^3}{3} f_s(p,t)(v_1 - v_2) . \qquad (3)$$

For monoenergetic injection (at the shock front) at momentum p_0, there is a source term of the form $Q\delta(p - p_0)$. Particles are also advected out of the acceleration region at speed v_2 so that particle conservation gives the equation

$$\frac{\partial}{\partial t} \left[4\pi^2 f_s L \right] = -\frac{\partial \Phi}{\partial p} - v_2 4\pi p^2 f_s + Q\delta(p - p_0) . \qquad (4)$$

Equation (4) is only valid in the absence of radiative losses, which will be negligible for the electrons responsible for radio emission in young supernovae, but such losses can also be included (Drury et al. 1999). When L is constant (which is not assumed in our numerical calculations) we have

$$\frac{\partial f_s}{\partial t} = -\frac{p}{t_a} \frac{\partial f_s}{\partial p} - \frac{q}{t_a} f_s + \frac{Q\delta(p - p_0)}{4\pi p^2 L} , \qquad (5)$$

where $t_a \equiv 3L/(v_1 - v_2)$ is the acceleration timescale and $q \equiv 3v_1/(v_1 - v_2)$. For momenta away from injection (i.e. for $p > p_0$), and in the steady state, the solution to equation (5) is $f_s \propto p^{-q}$ as in the analytic test particle treatment of diffusive shock acceleration.
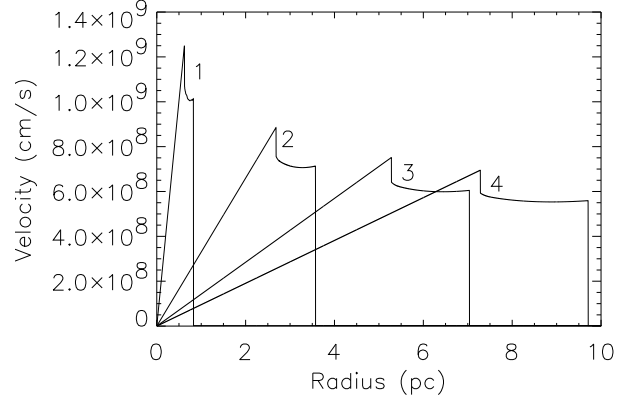
The shock accelerated particles are ultimately advected away from the acceleration zone, and the dominant processes are then advection with the local fluid flow and adiabatic losses. The downstream distribution, $f(\mathbf{r}, p, t)$, therefore evolves according to

$$\frac{\partial f}{\partial t} + \mathbf{v} \cdot \nabla f - \frac{1}{3}\nabla \cdot \mathbf{v} p \frac{\partial f}{\partial p} = 0 \qquad (6)$$

which is to be solved subject to the boundary condition $f(\mathbf{r_s}, p, t) = f_s(p, t)$.

4 Numerical solution and results

Starting from the onset of electron injection at time t_0, flow data are extracted from the hydrodynamical results and used to calculate the electron distribution. The acceleration and transport calculations thus introduce four model parameters: t_a, t_0, Q and p_0. The explicit numerical method for the hydrodynamics is necessarily stable and therefore satisfies the Courant-Friedrich-Lewy stability condition. However, the data for the calculation of the electron distribution are not usually extracted on the finest spatial and temporal scales used in the hydrodynamical calculations, which covers some ten to fifteen thousand cells in space. The data extracted from the hydrodynamical results could be at such a coarse resolution that any *explicit* numerical method for the electron acceleration and transport, used on that reduced data set, could be unconditionally unstable. We therefore use an *implicit* numerical method for the spatial part of the electron transport.

Introducing a new independent variable $y \equiv \ln(p/p_0)$ and defining $g_s(p, t) = p^{q_0} f_s(p, t)$, where $q_0 = 3v_1(t_0)/[v_1(t_0) - v_2(t_0)]$, equation (5) becomes

$$\frac{\partial g_s}{\partial t} = -\frac{1}{t_a} \frac{\partial g_s}{\partial y} + (q_0 - q) g_s + \frac{Q\delta(p - p_0)}{4\pi p^2 L} . \qquad (7)$$

We use an explicit upwind scheme to solve equation (7), which introduces a lower limit on the cell width in the variable y given by $\Delta y = \max(\Delta t)/t_a$, where $\max(\Delta t)$ is
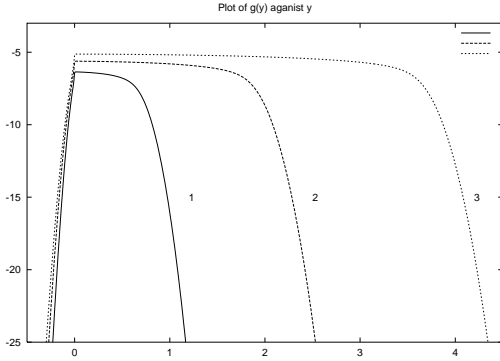
Fig. 5. The energetic electron distribution, multiplied by p^4 and integrated over the entire downstream region, as a function of y for an explosion in a constant density medium, at 1: $t_1 = 46$ yr, 2: $t_2 = 121$ yr and 3: $t_3 = 232$ yr. The acceleration time is $t_a = 25$ yr and injection is switched on at $t_0 = 4$ yr.
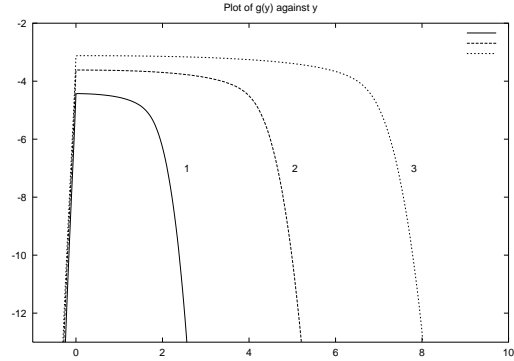
Fig. 6. The energetic electron distribution, multiplied by p^4 and integrated over the entire downstream region, as a function of y for an explosion into a circumstellar wind with density $\propto r^{-2}$, at 1: $t_1 = 129$ yr, 2: $t_2 = 279$ yr and 3: $t_3 = 447$ yr. The acceleration time is $t_a = 25$ yr and injection is switched on at $t_0 = 11$ yr.

the largest timestep provided from the hydrodynamical data. The spectrum can therefore only be resolved to an acceptable level of accuracy if the acceleration timescale is several times greater than the typical timesteps used in the hydrodynamical calculations. For SN1987A, where t_a is of the order of 10 to 100 days, this is an acceptable constraint.

Downstream of the shock equation (6) becomes

$$\frac{\partial f}{\partial t} = -v \frac{\partial f}{\partial r} - v_y \frac{\partial f}{\partial y} \tag{8}$$

when spherical symmetry is assumed, and the advection speed in logarithmic momentum space is given by

$$v_y = -\frac{1}{3r^2} \frac{\partial r^2 v}{\partial r} . \tag{9}$$

The condition $f(r_s(t), y, t) = f_s(y, t)$ represents the fact that the shock leaves an accelerated spectrum of particles in its wake. We solve equation (8) using a method which is explicit in momentum, and which does not impose a more stringent stability condition than that already required by the acceleration calculation. However, since data will in general be extracted from the highly spatially resolved hydrodynamics at much lower resolution, it is necessary to use semi-implicit differencing in the radial coordinate. This makes the code unconditionally stable in space and thus quite robust.

Initial results for an explosion in a constant density medium and in a stellar wind are shown in figures 5 and 6 which show the energetic particle distribution, $p^4 f(r, p, t)$, integrated over the entire downstream region, at three different epochs. The data used to produce figure 5 had twice as large a timestep as those used to generate figure 6. There are no artifacts in the plots to suggest that the acceleration code is being affected by the coarseness of the grid. At momenta extending upwards from the injection momentum, p_0, the computed spectrum initially shows the expected agreement with the analytic result for acceleration at a strong shock of compression ratio of four, i.e. $f(p) \propto p^{-4}$. The computed spectrum falls rapidly

below the asymptotic power law beyond a cutoff momentum which increases with the time since acceleration began. Below the injection momentum particles suffer adiabatic losses – which are quite small due to the limited time covered by these calculations – indicated by the fact that the distribution is non-zero for a narrow range of momenta below p_0.

5 Conclusions

We have presented initial calculations of energetic electron distributions using the results of hydrodynamical calculations in one spatial dimension. These results demonstrate a solution of the test particle acceleration and transport problem, using data from detailed hydrodynamical simulations, which takes just minutes to run on a PC. Applications of our method to more complicated models for supernova ejecta will facilitate the calculation of model radio synchrotron light curves and synthetic radio images, and will help to bridge the gap between sophisticated hydrodynamical simulations and detailed radio observations.

References

Ball, L., Kirk, J.G., ApJ, 396, L42-45, 1992
Blondin, J.M., Lundqvist, P., ApJ, 405, 337-352, 1993
Chevalier, R.A., ApJ, 258, 790-797, 1982
Colella, P., Woodward, P.R., J. Comp. Phys., 54, 174, 1984
Drury, L.O'C., Duffy, P., Eichler, D., Mastichiadis, A., Astron. Astrophys., 347, 370-374, 1999
Duffy, P., Ball, L., Kirk, J.G., ApJ, 447, 364-377, 1995
Dwarkadas, V.V., ApJ, 541, 418-427, 2000
Jun, B., Jones, T.W., ApJ, 511, 774-791, 1999
Luo, D., McCray, R., Slavin, J., ApJ, 430, 264-276